

Sorption and Transport of Gases in Miscible Poly(Methyl Acrylate)/Poly(Epichlorohydrin) Blends

J. S. CHIOU, J. W. BARLOW, and D. R. PAUL, *Department of Chemical Engineering and Center for Polymer Research, University of Texas, Austin, Texas 78712*

Synopsis

The sorption and the transport of He, Ar, N₂, CH₄, and CO₂ in miscible poly(methyl acrylate)(PMA)/poly(epichlorohydrin)(PECH) blends from 1 to 20 atm at 35°C are reported. For He, Ar, N₂, and CH₄, the permeabilities and the diffusion time lags are independent of the upstream pressure, if the compaction effect resulting from compression of the polymer membrane onto the supporting medium is eliminated. The permeability of CO₂ increases with upstream pressure but solubility follows a simple Henry's law behavior. For all five gases, the dependence of solubility, diffusion coefficient, and permeability on blend composition are compared with theoretical mixing rules with the conclusion that both the interaction energy density and the excess activation energy for gas diffusion in the blends are near zero. The fact that the specific volumes of the blends exactly follow linear additivity also confirms that only very weak interactions exist between PMA and PECH.

INTRODUCTION

Relatively few studies of sorption and transport of small molecules in polymer blends have appeared in the past decade considering the rapid growth during this period of the literature on polymer blends.¹ However, several early reports by Shur and Ranby²⁻⁷ contrasted the difference between the mixing rules for gas transport in miscible and immiscible blends. For immiscible blends, an S-shaped curve is usually observed when the logarithm of the gas permeability is plotted vs. blend composition, which is easily understood by appropriate application of Maxwell's equation or other similar relations for multiphase systems.^{8,9} For miscible blends, on the other hand, linear relations between the logarithm of gas permeability, P , and blend composition have been found^{2,3}, i.e.,

$$\ln P = \phi_1 \ln P_1 + \phi_2 \ln P_2 \quad (1)$$

where ϕ_1 and ϕ_2 are the volume fractions of component 1 and 2 in the blend. However, this relation was not given any theoretical foundation until recently. Paul has derived mixing rules for transport of gases in multicomponent polymers and showed that eq. (1) is a special case of more general mixing rules applicable only under certain conditions.¹⁰

It should be pointed out here that sorption and transport of small penetrants in miscible polymer blends are often complicated by the following which must be considered before interpreting plots of any coefficients or

parameters vs. blend composition. First, the observation temperature may be below the glass transition for one component of a blend and above the glass transition for the other component with the result being for a miscible system that the mixture is glassy over a portion of the composition range and rubbery over the remainder. It is well known that the mechanisms for sorption and transport in rubbers and glasses differ rather significantly and different models are needed to describe their behavior.¹¹ Second, one or both components may be crystalline with the result being that the fraction of the mixture which is amorphous varies with blend composition. Furthermore, the composition of the amorphous phase, where all sorption and transport occurs, will not be the same as the overall composition of the blend when a portion of one component is removed to form a crystalline phase.¹² Third, the permeability and solubility coefficients may depend on pressure or concentration in a variety of ways^{13,14} and care must be exercised in selecting a common basis for comparison of one blend composition with another. A useful approach in such cases^{15,16} is to employ an appropriate model from which pressure or concentration independent parameters can be deduced and then examine mixing rules for these parameters.

To test the mixing rules for gas sorption and transport in a miscible polymer blend system in the absence of some of the complexities mentioned above, the poly(methyl acrylate)/poly(epichlorohydrin) blend system is a good candidate. PMA and PECH are miscible as concluded from the single composition dependent glass transition temperature shown for the blend¹⁷ in Figure 1. Because both polymers are amorphous and rubbery, their blends are also amorphous and rubbery. Thus, no variation of the sorption or the transport mode occurs as blend composition varies. The purpose of this study is to measure the solubility, diffusion coefficient, and permeability of He, Ar, N₂, and CH₄, as well as CO₂ in these blends, and then to examine how their dependence on blend composition compares with mixing rules developed previously.¹⁰

BACKGROUND

The sorption of a simple gas in a rubbery and amorphous polymer can be described by Henry's law

$$C = k_D p \quad (2)$$

where C is gas concentration in the polymer phase, p is the pressure in the gas phase, and k_D is a solubility coefficient. Theoretically, the solubility coefficient can be determined from a single equilibrium sorption measurement or, more accurately, from the slope of a complete sorption isotherm. However, for some gases, the low amount of sorption in rubbery polymers often makes accurate measurement of sorption very difficult. Therefore, an indirect but convenient method is to use the transient permeation technique. In this approach, the permeability coefficient is measured in the steady state while the diffusion coefficient, if it is concentration independent, can be deduced from the diffusion time lag, θ , which is characteristic of the time to reach steady state, using

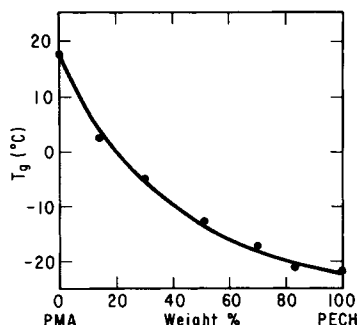


Fig. 1. Glass transition data by DSC for PMA/PECH blends.

$$D = l^2/6\theta \quad (3)$$

Thus, the solubility coefficient, k_D , is simply calculated from

$$P = k_D D \quad (4)$$

This approach has been extensively used for studying sorption and transport of gases in rubbery polymers, because P , D , and k_D can be obtained simultaneously from one single transient permeation experiment. However, one premise of this approach, i.e., a concentration-independent diffusion coefficient, may not always be met even for gases such as CO_2 . In these cases, the diffusion coefficient is often found to be an exponential function of concentration, i.e.,

$$D = D_0 \exp(\beta C) \quad (5)$$

where D_0 is the limiting diffusion coefficient at zero concentration, and β is a characteristic constant for the gas-polymer pair. The permeability for this case has been shown by Stern and Saxena¹⁸ to be given by

$$P = D_0[\exp(\beta k_D p_2) - 1]/\beta p_2 \quad (6)$$

when the solubility coefficient, k_D , is independent of concentration and the downstream pressure is zero.

From ternary solution theory,^{1,15,16} the solubility coefficient of a penetrant in a blend can be related to those in the constituent polymers by

$$\ln k_D = \phi_1 \ln k_{D1} + \phi_2 \ln k_{D2} + (BV_3/RT)\phi_1\phi_2 \quad (7)$$

where B is the binary interaction energy density between polymer 1 and 2 and V_3 is the molar volume of the penetrant. This equation has been used,^{15,16,19} to determine the interaction energy densities from measured solubility coefficients for the blend.

From the activated state theory of diffusion, the diffusion coefficient for a penetrant in a miscible blend can be related to those in the component polymers by the following¹⁰

$$\ln D = \phi_1 \ln D_1 + \phi_2 \ln D_2 + (aRT - 1)\Delta E_{12}/RT \quad (8)$$

where a is a constant and ΔE_{12} is the excess activation energy for diffusion in the blend. Combining eqs. (7) and (8), the permeability of a penetrant in a blend can be expressed by

$$\ln P = \phi_1 \ln P_1 + \phi_2 \ln P_2 + (BV_3/RT)\phi_1\phi_2 + (aRT - 1)\Delta E_{12}/RT \quad (9)$$

Thus, eq. (1) can be seen as the special case when the sum of the last two terms on the right-hand side of eq. (9) is zero.

Another approach to a mixing rule for gas permeability in blends has been based on a relation between the permeability coefficient and the free volume found by Lee.²⁰ If the free volume of the blend is assumed to be a linearly additive sum of those for the constituent polymers, the mixing rule for the permeability coefficient becomes

$$\ln(P/A) = [\phi_1/\ln(P_1/A) + \phi_2/\ln(P_2/A)]^{-1} \quad (10)$$

where A is a parameter in the Lee correlation specific for the particular penetrant. This equation can also be reduced to eq. (1) if $\ln A \gg \ln P_i$ or when P_1 and P_2 are similar in magnitude. If there is a volume change on mixing, the assumption about additivity of free volume does not hold and correction for this fact must be added.¹⁰

EXPERIMENTAL

The poly(methyl acrylate) was supplied by the courtesy of Celanese Chemical Company. It has a T_g of 18°C by DSC and $M_w = 576,000$ as measured by solution viscosity.²¹ The poly(epichlorohydrin) is a commercial product from B. F. Goodrich Company designated as Hydrin 100. This polymer has a T_g of -22°C by DSC. Both polymers are in the rubbery state at the experimental temperature of 35°C and are totally amorphous.

Membranes of PMA, PECH, and their blends having weight ratios of 75/25, 50/50, and 25/75 were prepared as follows. Homogeneous solutions were prepared by dissolving both polymers in hot toluene with vigorous stirring. Because both PMA and PECH have T_g 's below room temperature and are amorphous, their membranes are soft and sticky. For the purpose of easily releasing membranes from the casting surface, the polymer solution was poured onto a nonsticking cooking pan placed on a mercury pool to maintain a horizontal casting plane. After the solvent was slowly evaporated at ambient conditions, the membrane was further dried in an oven at 75°C for one day and then at 110–120°C for another 1–2 days. To release the membrane from the pan, the latter was placed on dry ice for about 10 min to stiffen the membrane so it could be peeled off. Finally, the membrane was cut to the desired shape. The thickness of the membrane was gauged by a micrometer with an accuracy of 0.001 mm. For CO₂ sorption experiments, membranes were cast on flat aluminum foil. After the same drying procedures described above, the membrane, still adhered to the aluminum foil, was cut into strips, coiled, and inserted into the sorption cell. The volume

of the aluminum was subtracted from the dead volume of the sorption cell in obtaining the sorption isotherm.

The apparatus and the experimental techniques used in this study were the same as those described earlier.²² Gas sorption experiments were done in a dual volume cell where the amount of gas sorbed by the polymer was monitored by pressure transducers. In the gas permeation experiments, the membrane was sealed on a porous stainless steel disc which divides the cell into upstream and downstream sides.

Densities of the polymers were measured at 30°C using a density gradient column based on aqueous solutions of calcium nitrate. The density data were also used to calculate the membrane thickness. The agreement between this calculated thickness and that measured by the micrometer was usually within 2%.

RESULTS AND DISCUSSION

Density

The densities and the specific volumes of PMA, PECH, and their blends are plotted vs. the weight fraction of PECH in Figure 2. While the density curve has a small negative deviation from the tie line, the specific volumes follow very closely the line of linear volume additivity. In fact, the line shown is the best linear fit to the data. The upper part of Figure 2 shows, on a greatly expanded scale a residual plot, i.e., experimental values relative to those calculated from the regression line. There is no apparent systematic trend in the residual which suggests that the volume change on mixing is less than the error in these specific volume measurements which is less than 10^{-3} cm³/g. This implies that the interaction between PMA and PECH is not large.

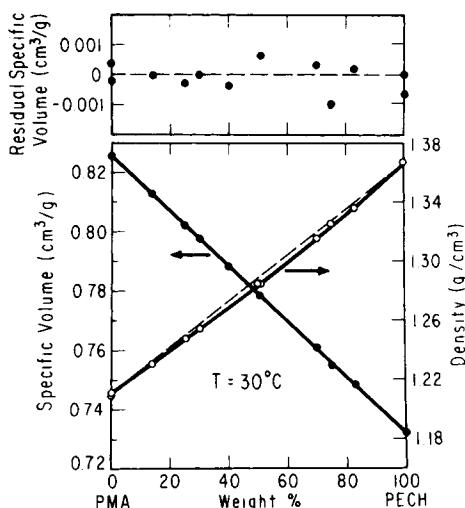


Fig. 2. Densities and specific volumes of PMA/PECH blends at 30°C. Upper part shows residual plot on expanded scale.

Sorption and Transport of He, Ar, N₂ and CH₄

The permeabilities of these four gases were preliminarily studied using randomly chosen upstream pressures ranging from 1 to about 20 atm. The results showed that the gas permeability at lower pressures could not be reproduced and appeared to be decreased by as much as 10–20% once the membrane was exposed to high upstream pressures such as 20 atm. To illustrate this effect in a systematic manner, the upstream pressure was sequentially increased from 1–20 atm and then recycled. Figure 3 is a typical result showing that the apparent permeability of Ar in PECH decreases with upstream pressure, while the diffusion time lag increases. In the first cycle, the permeability decreases 20% as the upstream pressure increases from 1 to 20 atm while the time lag increases 12%. In the second cycle, almost parallel curves to the first cycle are observed, except that the permeability is smaller and the time lag is larger than in the first cycle at the same pressure. Similar results are observed for PMA and PMA/PECH blends, but the extents of the decrease in permeability and the increase in the time lag become less as the content of PMA in the membrane increases. Figure 4 shows that the permeability of Ar in PMA is reduced 12%, whereas the time lag increases 6% for the 1 ~ 20 atm upstream pressure variation in the first cycle.

A filter paper with negligible resistance to gas transport is placed between the membrane and the sintered stainless steel support disk as a cushion (see inset in Figs. 3 and 4). The filter paper (Whatman, Qualitative 1) is softer and has finer pores than the sintered stainless-steel disk. After being subjected to a pressure as low as 1 atm on the upstream side of the permeation cell, the membrane was found to stick to the filter paper and could not be peeled off. This suggests that compaction of the elastomeric membranes into the pores of the supporting filter paper occurs which would increase the actual gas transport path and in turn decrease the permeation rate and increase the diffusion time lag. The fact that results for PECH

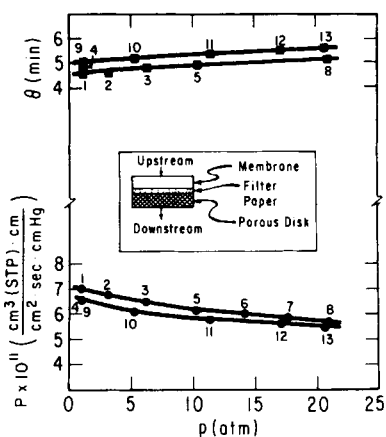


Fig. 3. Permeability and time lag data for Ar in PECH at 35°C. The numbers indicate the sequence of measurement. The insert shows the membrane-support assembly. Thickness is 4.8 mil.

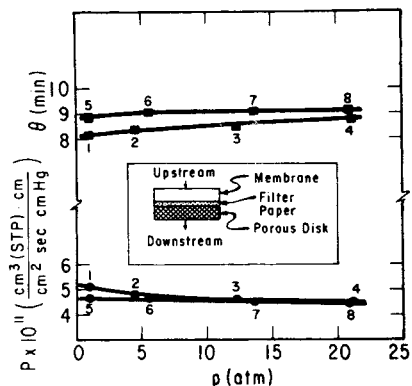


Fig. 4. Same as Figure 3, except the polymer is PMA. Ar in PMA at 35°C. Thickness is 4.84 mil.

are affected more than for PMA is in accord with this speculation, because the former is softer than the latter. Thus, without the filter paper the stainless-steel support disk would be irreversibly contaminated by these elastomers.

For all of the data reported here, the above mentioned problem was resolved by using the following two measures, simultaneously, to get near compaction-free results. The first was to use thick membranes (7–10 mils) since the relative contribution of the transport resistance at the membrane-filter paper interface will be less the thicker the membrane is. The second was to employ the lowest possible upstream pressure, about 1 atm, to minimize the force of compression. In fact, one can get compaction-free data by extrapolating the curves in Figures 3 and 4 to zero pressure. However, these results differ from those at 1 atm by less than 2% so that all the data presented and compared in this section, unless otherwise specified, were obtained at 1 atm upstream pressure with the conventional membrane-support assembly.

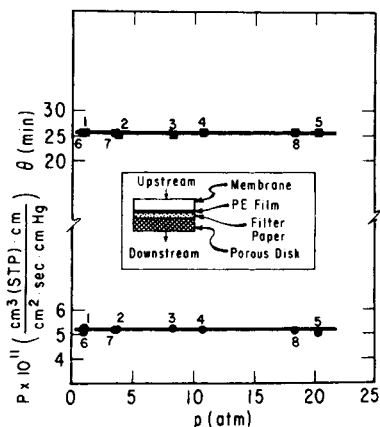


Fig. 5. Same as Figure 4, except the inset shows the modified membrane-support assembly. Thickness is 8.7 mil.

In the final stages of this work, a modified membrane-support assembly was devised which completely eliminates the compaction problem giving permeabilities and time lags completely independent of upstream pressure. In this assembly (see the inset in Fig. 5), a piece of thin polyethylene (PE) film about 0.5 mil thick is placed between the elastomeric membrane and the supporting filter paper. Obviously, the PE film prevents the membrane from contacting or being compressed into the pores of the filter paper. The gas transport resistance in the PE film is negligible compared with that for PMA/PECH membranes. This can be seen from the following equation²³

$$l/P = l_1/P_1 + l_2/P_2$$

where l is thickness. Designating the PE layer as 2, we have typically $l_1 = 15 \sim 20 l_2$, and $P_2 = 11 \sim 14P_1$ since the measured N_2 permeability in PE film is 2.6 Barrer whereas those for PMA and PECH are 0.19 and 0.24 Barrer, respectively. Thus, the gas transport resistance in the PE film, l_2/P_2 , is only 0.4 ~ 0.6% of that in the PMA/PECH membrane, l_1/P_1 , which is negligible considering other sources of error.

Figure 5 shows that the permeability and the time lag for Ar in PMA are essentially independent of the upstream pressure when the compaction problem is eliminated in this way. The permeability, 0.52 Barrer, is the same as that extrapolated to zero pressure in Figure 4. The time lag of 25.6 min in Figure 5 at the thickness of 8.7 mil can be scaled by the l^2 factor to be 7.9 min at the same thickness as in Figure 4, 4.84 mil. The difference between this rescaled time lag, and that extrapolated from Figure 4, 8.1 min, is within the limits of experimental error.

TABLE I
Permeability, Diffusion, and Solubility Coefficients for He, Ar, N_2 , and CH_4 in PMA/PECH Blends at 35°C

		PMA	75 PMA/ 25 PECH	50 PMA/ 50 PECH	25 PMA/ 75 PECH	PECH
He	P^a	10.6	9.04	7.45	6.14	4.83
	D^b	788	715	654	—	488
	k_D^c	1.35	1.26	1.14	—	0.990
Ar	P	0.511	0.547	0.591	0.660	0.710
	D	5.13	5.95	6.77	7.92	9.18
	k_D	9.96	9.19	8.73	8.33	7.73
N_2	P	0.187	0.192	0.212	0.237	0.240
	D	3.85	4.42	5.08	5.95	6.55
	k_D	4.86	4.34	4.17	3.98	3.66
CH_4	P	0.235	0.294	0.402	0.548	0.657
	D	1.21	1.67	2.42	3.33	4.22
	k_D	19.4	17.6	16.6	16.4	15.6

$$^a P[=] 10^{-10} \frac{\text{cm}^3(\text{STP}) \cdot \text{cm}}{\text{cm}^2 \cdot \text{s} \cdot \text{cmHg}}$$

$$^b D[=] 10^{-8} \frac{\text{cm}^2}{\text{s}}$$

$$^c k_D[=] 10^{-4} \frac{\text{cm}^3(\text{STP})}{\text{cm}^3(\text{polym}) \cdot \text{cmHg}}$$

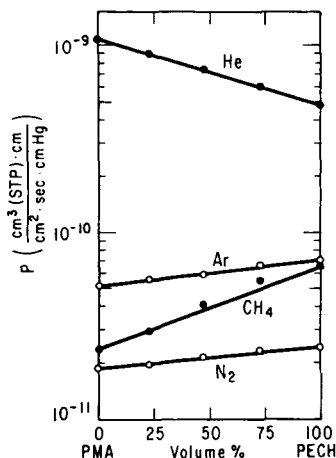


Fig. 6. Semilogarithmic plots of permeabilities vs. vol % of PECH in blends. $T = 35^{\circ}\text{C}$.

The permeability, solubility, and diffusion coefficients for He, Ar, N₂ and CH₄ in the PMA/PECH membranes are listed in Table I. The logarithms of the three coefficients are plotted vs. the volume fraction of PECH in Figures 6–8, respectively, to establish the mixing rules for gas sorption and transport in these polymer blends. Within the limit of experimental errors (about 3%) no deviations from linear additivity are seen. Consequently, the excess terms in eqs. (7)–(9) must be of the same magnitude or less than the experimental errors in the measured data.

Sorption and Transport of CO₂

The permeability of CO₂ in PMA/PECH blends increases with the upstream pressure as shown in Figure 9 where measurements were made by increasing the upstream pressures sequentially from 1–20 atm. Increasing permeability with pressure seems to be a general transport property of CO₂

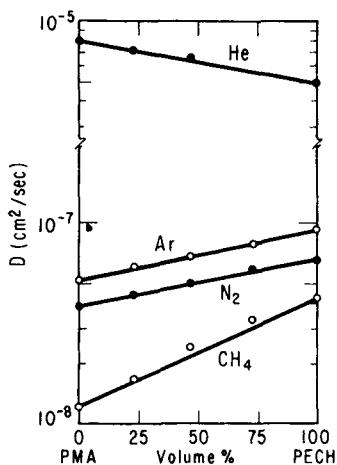


Fig. 7. Semilogarithmic plots of diffusion coefficients vs. vol % of PECH in blends. $T = 35^{\circ}\text{C}$.

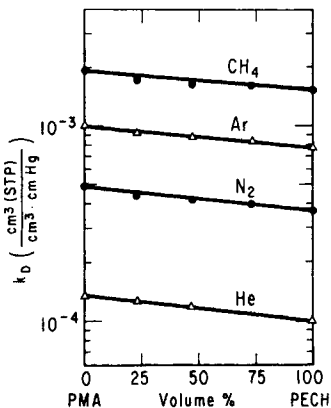


Fig. 8. Semilogarithmic plots of solubilities vs. vol % of PECH in blends. $T = 35^{\circ}\text{C}$.

in rubbery polymers. Other polymers, such as a copolymer of vinylidene chloride and vinyl chloride, poly(vinylidene fluoride), poly(vinyl acetate), and poly(ϵ -caprolactone) examined recently in this laboratory and polyethylene studied by others^{24,25} also show this behavior. This phenomenon is generally explained by an exponentially increasing diffusion coefficient with penetrant concentration. If the solubility coefficient of the gas is assumed to be independent of the concentration, the permeability will be a function of three parameters, D_0 , β , and k_D as seen by eq. (6). Theoretically, these three parameters can all be obtained by the fitting of one set of permeability versus pressure data to this equation by regression analysis. This approach, however, was not used here. Instead, the solubility coefficient was measured directly using the dual volume sorption cell; and thus, only the other two parameters, D_0 and β must be deduced by regression of the transport data. There are two reasons for doing so. First, the assumption of concentration-independent solubility coefficients should be tested. Second, this makes determination of the transport parameters more reliable.

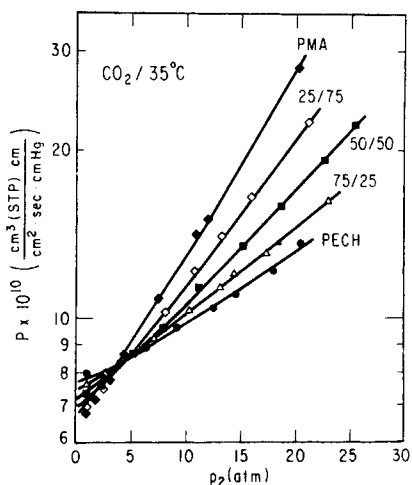


Fig. 9. Semilogarithmic plots of CO_2 permeabilities vs. pressure at 35°C . The solid lines are calculated using eq. (6) and the data from Table II.

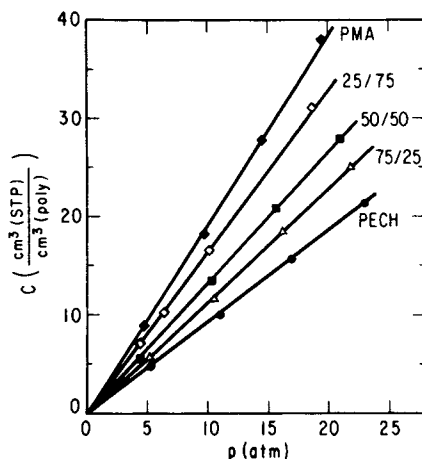


Fig. 10. Sorption isotherms for CO_2 in PAM/PECH blends at 35°C .

The sorption isotherms for CO_2 in PMA/PECH mixtures are shown in Figure 10. Obviously, Henry's law is followed. The solubility coefficients calculated from the slopes are listed in Table II, and their logarithms are plotted versus the volume fraction of PECH in Figure 11. In Figure 11, the deviations from the tie line are no more than 2%, which is within experimental error.

For each blend, the value of k_D listed in Table II is used in conjunction with eq. (6) to find values of D_0 and β by computer regression analysis. These results are also included in Table II. As seen in Figure 9, the experimental permeabilities are fitted well by eq. (6). Deviations between the measured permeabilities and the calculated permeabilities average about 2%. These results confirm that the increasing permeability of CO_2 in PMA/PECH blends originates from an exponentially increasing diffusion coefficient with concentration. The logarithm of D_0 is plotted vs. the PECH volume fraction in Figure 12, and a linear tie line represents the results quite well which corresponds to the limiting case of eq. (8) when the excess term, $(aRT - 1)\Delta E_{12}/RT$, is essentially zero. As seen in Table II, the value of β does not vary significantly with blend composition. The fact that the CO_2 permeability increases much faster in PMA than in PECH is primarily because the former has a solubility coefficient more than a factor of two

TABLE II
Sorption and Transport Parameters for CO_2 in PMA/PECH Blends at 35°C

	k_D , $\frac{\text{cm}^3(\text{STP})}{\text{cm}^3(\text{poly}) \cdot \text{atm}}$	D_0 , $10^{-8} \frac{\text{cm}^2}{\text{s}}$	β , $\frac{\text{cm}^3(\text{polym})}{\text{cm}^3(\text{STP})}$
PMA	1.981	2.56	0.0605
25/75	1.708	3.03	0.0570
50/50	1.374	3.88	0.0569
75/25	1.153	4.86	0.0540
PECH	0.946	6.09	0.0542

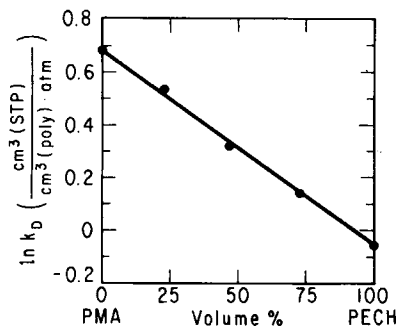


Fig. 11. Logarithms of CO₂ solubilities vs. blend composition at 35°C.

larger than that for the latter rather than because of slight differences in β . The leveling off of permeability at low pressure is predicted by eq. (6) and has been observed for the transport of CO₂ in poly(vinyl acetate).²⁶

It is also of interest to rationalize the CO₂ gas permeability in blends with that predicted by the free volume mixing rule given by eq. (10). Because the CO₂ permeabilities depend on pressure and the dependency varies from one polymer to another, only the zero pressure permeabilities are chosen for comparison. The *experimental* values of P_0 were calculated from $P_0 = k_D D_0$. As seen in Table III, the experimental P_0 's are quite close to those predicted by eq. (1). Because the P_0 values for PMA and PECH are so close, eq. (10) gives predictions identical to those from eq. (1). Note that for CO₂, A is 6×10^{-6} cm³(STP) cm/s cm²cmHg.¹⁰ When P_1 and P_2 are substantially different, eq. (10) predicts values higher than given by eq. (1).

CONCLUSIONS

The nonreproducible and apparent pressure dependent permeabilities and diffusion time lags for He, Ar, N₂, and CH₄ in these elastomeric membranes observed using a conventional membrane-support assembly have been shown to result from the compaction or flow of the membrane into the pores of the supporting filter paper. A modified membrane-support assembly, which sandwiches a very thin PE film between the polymer mem-

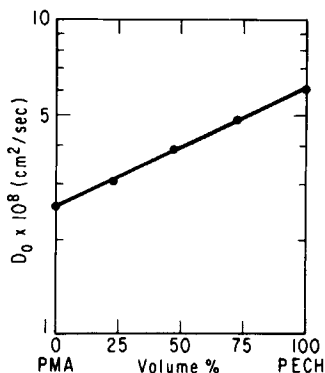


Fig. 12. Semilogarithmic plots of CO₂ diffusion coefficients at zero concentration vs. volume % of PECH at 35°C.

TABLE III
Comparison of Zero Pressure Permeabilities for CO₂ in PMA/PECH blends at 35°C with
Mixing Rules

	$P_0 = k_D D_0^a$	P_0 by eq. (1)	P_0 by eq. (10)
PMA	6.67	—	—
25/75	6.81	6.88	6.87
50/50	7.02	7.10	7.09
75/25	7.37	7.33	7.32
PECH	7.58	—	—

^a All permeabilities are in units of Barrers.

brane and the supporting filter paper, can eliminate this problem and give reliable permeability and time lag data for elastomeric materials.

In contrast to the results for He, Ar, N₂, and CH₄, the permeability of CO₂ in these materials increases with upstream pressure. This is caused by a concentration dependent increase of diffusion coefficient since the solubility coefficient was found to be independent of the equilibrium sorption pressure. An exponentially increasing diffusion coefficient with the concentration is found to fit the permeability data well.

Solubilities, diffusion coefficients, and permeabilities for the five gases in PMA/PECH blends were found to follow a simple additivity rule within the limit of experimental errors. This along with the linear additivity of specific volumes indicate that the binary interaction energy density, B , and the excess activation energy of gas diffusion, ΔE_{12} , in PMA/PECH blends are quite small. This is consistent with inverse gas chromatography results for this blend system reported recently.²⁷

It is instructive to compare the permeabilities measured here for the pure components, PMA and PECH, with those reported in the literature where possible. For PMA, the present data agree rather closely with that reported by Burgess, Hopfenberg, and Stannett.²⁸ On the other hand, our data for PECH show considerably higher permeabilities than those listed in a trade publication.²⁹ While not specified, the latter probably refer to commercially compounded materials containing large amounts of filler which would account for this difference. It is significant to note that for most gases, PMA and PECH are much less permeable than butyl rubber^{30,31} which is noted for its barrier characteristics—butyl rubber is about three times more permeable to nitrogen gas. Thus, these blends might be especially useful for applications where good barrier properties are required.

This research was supported by the U.S. Army Research Office.

References

1. H. B. Hopfenberg and D. R. Paul, *Polymer Blends*, Vol. I D. R. Paul and S. Newman, Eds., Academic, New York, 1978, Chap. 10.
2. B. G. Ranby, *J. Polym. Sci. Symp.* **51**, 89 (1975).
3. Y. J. Shur and B. Ranby, *J. Appl. Polym. Sci.*, **19**, 1337 (1975).
4. Y. J. Shur and B. Ranby, *J. Appl. Polym. Sci.*, **19**, 2143 (1975).
5. Y. J. Shur and B. Ranby, *J. Appl. Polym. Sci.*, **20**, 3105 (1976).
6. Y. J. Shur and B. Ranby, *J. Appl. Polym. Sci.*, **20**, 3121 (1976).
7. Y. J. Shur and B. Ranby, *J. Macromol. Sci. Phys.*, **B14**, 565 (1977).

8. L. M. Robeson, A. Noshay, M. Matzner, and C. N. Merriam, *Die Angew. Makromol. Chem.* **29/30**, 47 (1973).
9. A. E. Barnabeo, W. S. Creasy, and L. M. Robeson, *J. Polym. Sci., Polym. Chem. Ed.*, **13**, 1979 (1975).
10. D. R. Paul, *J. Membr. Sci.*, **18**, 75 (1984).
11. D. R. Paul, *Ber. Bunsenges. Phys. Chem.*, **83**, 294 (1979).
12. W. E. Preson, J. W. Barlow, and D. R. Paul, *J. Appl. Polym. Sci.*, **29**, 845 (1984).
13. D. R. Paul and W. J. Koros, *J. Polym. Sci., Polym. Phys. Ed.*, **14**, 675 (1976).
14. J. S. Chiou, Ph.D. dissertation, University of Texas at Austin, 1984.
15. P. Masi, D. R. Paul, and J. W. Barlow, *J. Polym. Sci., Polym. Phys. Ed.*, **20**, 15 (1982).
16. G. Morel and D. R. Paul, *J. Membrane Sci.*, **10**, 273 (1982).
17. A. C. Fernandes, J. W. Barlow, and D. R. Paul, to be published.
18. S. A. Stern and V. Saxena, *J. Membr. Sci.*, **7**, 47 (1980).
19. H. G. Spencer and J. A. Yavorsky, *J. Appl. Polym. Sci.*, **28**, 2937 (1983).
20. W. M. Lee, *Polym. Eng. Sci.*, **20**, 65 (1980).
21. S. H. Goh, D. R. Paul, and J. W. Barlow, *Polym. Eng. Sci.*, **22**, 34 (1982).
22. W. J. Koros, D. R. Paul, and A. A. Rocha, *J. Polym. Sci., Polym. Phys. Ed.*, **14**, 687 (1976).
23. R. M. Barrer, *Diffusion in Polymers*, J. Crank and G. S. Park, Eds., Academic, New York, 1968, Ch. 6.
24. S. A. Stern, S. M. Fang, and R. M. Jobbins, *J. Macromol. Sci. Phys.* **B5**, 41 (1971).
25. S. A. Stern and S. M. Fang, *J. Polym. Sci. A2*, **10**, 201 (1972).
26. K. Toi, Y. Maeda, and T. Tokuda, *J. Membr. Sci.*, **13**, 15 (1983).
27. Z. Y. Al-Saigh and P. Munk, *Macromolecules*, **17**, 803 (1984).
28. W. H. Burgess, H. B. Hopfenberg, and V. T. Stannett, *J. Macromol. Sci. Phys.*, **B5**, 23 (1971).
29. E. Scheer, *The Vanderbilt Rubber Handbook*, R. O. Babbit, ed., R. T. Vanderbilt Company, Incorporated, Connecticut, 1978, p. 284.
30. G. J. van Amerongen, *J. Polym. Sci.*, **5**, 307 (1950).
31. G. J. van Amerongen, *J. Appl. Phys.*, **17**, 972 (1946).

Received June 14, 1984

Accepted October 15, 1984